Water Air Soil Pollut (2020) 231: 478
https://doi.org/10.1007/s11270-020-04853-y

Competitive Adsorption of As(III), As(V), and PO_4 by an Iron Oxide Impregnated Activated Carbon: Surface Complex Modeling

T. Angele Ngantcha-Kwimi · Brian E. Reed

Received: 30 June 2020 / Accepted: 27 August 2020 / Published online: 2 September 2020

Abstract The objective of this study was to predict the competitive adsorption of As(III), As(V), and PO_4 by an iron oxide impregnated carbon (L-Act, 9% Fe(III) amorphous iron oxide) over a range of environmental conditions using the surface complexation modeling (SCM) approach. L-Act surface complexation constants determined from a single pH-adsorption edge were used to predict pH-dependent competitive removal in singular, binary, and tertiary adsorbate systems. As(III), As(V), and PO_4 complexes were modeled as bidentate binuclear species at low pH and monodentate species at high pH using the two monoprotic surface site/diffuse electric double layer model (2MDLM). *F* values determined based on 2MDLM predictions were close to those calculated by FITEQL (a statistical optimization program) demonstrating the effectiveness of the 2MDLM in describing adsorption behavior. *F* values were generally in the recommended range of 0.1–20 indicating a good fit between the data and the model. The 2MDLM also successfully predicted As(III)/As(V)/PO_4 adsorption data of hydrous ferric oxide and goethite adsorbents from the literature.

Keywords Surface complexation modeling · Competitive adsorption · As(III) · As(V) · PO_4 · Iron impregnated activated carbon

1 Introduction

Arsenic is of a serious environmental concern due to its toxicity and carcinogenicity (Chen et al. 1994; Smith et al. 1992). Consequently, the US EPA has reduced the maximum contaminant level (MCL) of arsenic in drinking water from 50 to 10 μg/L with a goal of 0 μg/L (US EPA 2001). As(V) is predominant under oxidizing conditions and is generally better adsorbed than As(III), while As(III) occurs predominantly under reducing conditions, is more mobile in ground waters, and is 60 times more toxic than As(V) (Jain and Ali 2000). While the MCL is based on total arsenic, the difference in toxicity and chemical behavior requires that attention be paid to the fate of individual arsenic species in treatment systems.

The ability of iron oxides/hydroxides to remove As is well known (Dzombak and Morel 1990; Dixit and Hering 2003), but their use in fixed-bed columns is a challenging due to their small particle size, low hydraulic conductivity, and durability; thus, they have been impregnated onto more durable materials such as activated carbons, sand, and diatomite (Vaishya and Gupta 2003; Jang et al. 2006; Reed et al. 2000, Vaughan and

Electronic supplementary material The online version of this article (https://doi.org/10.1007/s11270-020-04853-y) contains supplementary material, which is available to authorized users.

T. A. Ngantcha-Kwimi
Consolidated Edison of New York, 5th Floor NW, 4 Irving Pl, New York, NY 10003, USA

T. A. Ngantcha-Kwimi (✉) · B. E. Reed
University of Maryland, Baltimore County, TRC Bldg, Rm 255A, Baltimore, MD 21250, USA
e-mail: angelekwimi@gmail.com

Reed 2005; Ngantcha et al. 2011). Iron oxide impregnated activated carbon, the study adsorbent in our work, is durable, could potentially allow the concurrent removal of organics and inorganics, and enjoys widespread familiarity with drinking water professionals (Reed et al. 2000; Vaughan and Reed 2005; Ngantcha et al. 2011). Iron oxide impregnated activated carbons are ideal for use by small communities and in point-of-use devices to treat arsenic contaminated water.

Isotherms are used to predict the relationship between aqueous and solid phase concentrations; however, they are not able to mechanistically account for changes in environmental conditions such as pH, adsorbate/adsorbent ratio, and the presence of competing ions (e.g., PO_4). In contrast, the surface complex model (SCM) assumes that surface sites interact with ions in a fashion similar to aqueous reactions; thus, mass action laws can be written describing the interactions between the surface and aqueous species (Dzombak and Morel 1990; Hayes et al. 1991). In theory, complexation constants determined from a single experiment can be combined to predict a competitive behavior over a range of environmental conditions. While As(V) and As(III) adsorption by iron-based sorbents has been modeled previously using the SCM approach, this study expands on the previous work by modeling competition in binary and for the first time in tertiary adsorbate systems. The SCM approach can be used to evaluate the effect of feed water characteristics on arsenic removal by iron-based adsorbents and can also be combined with a mass transport model to predict the dynamic behavior of arsenic in natural and treatment systems (Vaughan et al. 2007; Smith 1998).

In this study, we seek to predict the competitive adsorption of As(III), As(V), and PO_4 by an iron oxide impregnated carbon (L-Act) over a range of environmental conditions. Specific objectives are as follows: (1) develop pH-dependent adsorption data for As(III) for a range of adsorbent/adsorbate ratios, (2) determine L-Act surface complexation constants from a single As(III)/L-Act pH-adsorption edge, (3) combine As(III) surface complexation constants with those in the literature for As(V) and PO_4 and predict competition in binary (As(III)–As(V), As(III)–PO_4) and tertiary (As(III)–As(V)–PO_4) adsorbate systems, and (4) determine to what extent the 2MDLM can predict arsenic removal for other iron oxide based adsorbents.

2 Materials and Methods

2.1 Adsorbent Characterization

The virgin granular activated carbon (Darco 2040) and iron oxide impregnated carbon (L-Act) were acquired from NORIT Americas, Inc. (Atlanta, Georgia). Ngantcha-Kwimi and Reed (2016) characterized Darco 2040 and L-Act and reported that the impregnation process increased the iron content from 0.15 to 9% and decreased the total surface area (650 to 590 m^2/g) and total pore volume (0.95 to 0.73 cm^3/g), while the pH_{zpc} was relatively unchanged (7.2 to 7.1). Given that the pH_{zpc} are so close, the iron oxide component would also have a similar pH_{zpc}. SEM-EDS and TEM-EDS confirmed the presence of Fe on L-Act, and XRD results indicated that the impregnated Fe(III) oxide was primarily amorphous.

2.2 Adsorption Experiments

As(III) adsorption as a function of pH was examined under equilibrium conditions at $I = 10^{-2}$ N (as $NaNO_3$) for varying amounts of L-Act and As(III). Adsorbents were crushed so that 100% passed through and were retained by 200-mesh (74 um) and 400-mesh (37 um) sieves, respectively. For As(III)-only experiments, concentrations of 0.0013 to 0.013 mM As(III) were examined, while for binary adsorbate tests, the following molar ratios were studied: As(III):PO_4 (1:0.5, 1:1, and 1:2) and As(III):A(V) (1:1, 1:1.5, 1:2, and 2:1). For tertiary adsorbate tests, As(III):As(V):PO_4 molar ratios of 1:1:1, 1:1:2, 1:3:6, and 1:0.3:1.7 were examined.

One-liter solutions at targeted molar ratios were prepared, and varying amounts of L-Act were added so that the adsorbent concentrations ranged from 0.03 to 0.225 g/L. Fifty mL aliquots of the solutions were withdrawn, dispensed into polypropylene vials and NaOH or HNO_3 (0.1 or 1 N) added to adjust the pH. All samples were placed on a tumbler for 48 h after which the slurry pH was measured; the samples were filtered through a 0.45-μM membrane filter, and the filtrate was analyzed for total As/P, As(III), and As(V).

2.2.1 As(III) Oxidation

As(III) can be oxidized to As(V) in the presence of activated carbon and the pH at which this reaction begins needs to be determined to accurately model As

adsorption (Ngantcha et al. 2011; Daus et al. 2004). L-Act was contacted with an As(III)-only solution for 2 days at pHs ranging from 7.4 to 9.6. The slurry was filtered (0.45 um) and the solids were captured. The As-loaded L-Act was digested with 10% HNO_3 in a serial fashion until the concentration of Fe in the HNO_3 extractant was < 1% of the total iron present. The serial extractant solutions were combined and analyzed for Fe and total As by ICP and As(III)/As(V) by IC-ICP. As/Fe concentrations from the original filtration step were also measured, and mass balances on Fe and As were conducted. Mass balances' closures were excellent, within $4.5 \pm 3.2\%$ for Fe and $7.3 \pm 4.5\%$ for As. A no-adsorbent As(III) control was carried through the process, and no oxidation of As(III) was observed over the pH range investigated.

2.3 Analytical Methods

Total As and P concentrations were measured using the inductively coupled plasma (ICP) (Agilent 7500 series), and [As(III)] and [As(V)] were measured by ion chromatography (IC) (ICS 2000 system) coupled with ICP (IC-ICP). The total arsenic measured by ICP was in excellent agreement with the sum of As(III) and As(V) determined by IC-ICP. A Dionex As18 column was used for the IC with sodium hydroxide as the mobile phase at a flow rate of 0.3 mL/min at ambient temperatures. The injection volume was set at 100 μL. A two-step gradient elution was employed in order to achieve the best possible separation of the arsenic species. The retention times were 7.85 and 14.11 min for As(III) and As(V), respectively. ICP analytical recoveries were conducted on about 7% of As samples (27 samples) and averaged 109.4%. Arsenic sample triplicates on about 12% of the samples (44 samples) had relative standard deviations ranging from 0.1 to 13.5%. PO_4 recoveries on about 6% of samples (12 samples) averaged 116%, and the relative standard deviations for PO_4 triplicates on about 9% of the samples (23 samples) ranged from 0.05 to 17%. Analytical recoveries were conducted on about 13% of samples (6 samples) and averaged 94%.

2.4 Surface Complexation Modeling Approach

Based on previous work (Vaughan and Reed 2005; Ngantcha et al. 2011; Ngantcha-Kwimi and Reed 2016), L-Act acid-base behavior was modeled using the two monoprotic surface site representations and the diffuse layer electrostatic model (2MDLM). Historically, the surfaces of amphoteric adsorbents have been modeled as a single diprotic acid due to the ease of determining equilibrium parameters by graphical techniques. With the development of computer parameter estimation programs, other surface site representations can be used, such as multiple monoprotic sites (Vaughan and Reed 2005; Ngantcha et al. 2011; Ngantcha-Kwimi and Reed 2016; Reed and Matsumoto 1991). In the diprotic surface site representation, a single diprotic site can accept or release protons (Dzombak and Morel 1987). The monoprotic surface site representation assumes that the sites can independently accept or release protons. Vaughan and Reed (2005) illustrated the reactions, mass action laws, and mass balances that describe the monoprotic surface site representation. In these reactions, P^k and N^k are monoprotic surface sites carrying a positive and negative charge, respectively, and k is an index to differentiate between multiple positively and negatively charged sites. The surface must be represented by at least one of each type of site to account for the change of surface charge sign with pH (Vaughan and Reed 2005).

The 2-monoprotic acid site representation is mechanistically more suitable than the diprotic approach because a variety of OH groups exists on the iron oxide surface which vary in the number and arrangement of adjacent oxide ions (James and Parks 1982). The 2MDLM approach has also been demonstrated to better fit experimental data (Vaughan and Reed 2005; Ngantcha et al. 2011; Ngantcha-Kwimi and Reed 2016). The electric double layer that surrounds a hydrous solid can be described using different models that range in complexity from the simple diffuse layer model to the complex triple layer model. The diffuse layer model, used in this study for its simplicity, is applicable to low ionic strength settings and assumes chemisorption for sorbed ions (Westall and Hohl 1980) (inner sphere complexes) as is the case for this work. The diffuse layer model assumes that all specifically bound ions (H^+,OH^-) are bound to the inner o-layer, whereas all the background electrolytes (such as Na^+, NO_3^-) exist in in the diffuse (d) layer (Vaughan and Reed 2005; Dzombak and Morel 1987).

As(III) surface complexation constants were determined by FITEQL (Herbelin and Westall 1999) using the following inputs: aqueous As(III) speciation reactions (Eqs. 1, 2, and 3, Table 1), L-Act surface acid-base reactions (Eqs. 4 and 5), As(III) surface complexation

reactions (Eqs. 6, 7, and 8), and data from one As(III)-only pH-adsorption edge (0.013 mM As(III); 0.15 g/L L-Act). The basic principle of the surface complexation model assumes that sites on the surface interact with ions in a fashion similar to aqueous reactions; thus, mass action laws can be written describing the interactions between the surface and aqueous species (Dzombak and Morel 1990; Hayes et al. 1991). FITEQL is a non-linear least square optimization program that is commonly used to determine the optimal surface complexation equilibrium constants and the total chemical concentrations in an equilibrium problem. The retention of arsenic(III) and arsenic(V) at adsorption sites has been demonstrated to be predominantly by ligand exchange with OH-, and these have been studied broadly by X-ray adsorption fine structure (EXAFS) and infrared spectroscopy (Waychunas et al. 1993; Manceau 1995; Fendorf et al. 1997; Lumsdon et al. 1994). The release of OH during anion adsorption has also been demonstrated by Stumm (1995) and Jain et al. (1999). Surface complexation reactions were selected by comparing the speciation diagrams for aqueous As(III) and the L-Act surface (SI Fig. S1) under the criteria that its best to use the fewest number of reasonable reactions to attain the best fit. We assumed that H_3AsO_3 will preferentially exchange OH^- from the ≡NOH group at lower pH and at higher pH H_3AsO_3 and $H_2AsO_3^-$ will exchange OH^- from the ≡POH site (Table 1, Eqs. 6, 7, and 8).

At lower pH, a bidentate binuclear reaction was assumed for the ≡NOH site, and two monodentate reactions were used at higher pH for the ≡POH site which is consistent with literature results which report that As(III) sorbs on iron oxides by forming both bidentate binuclear and monodentate complexes (Manning et al. 1998; Ona-Guema et al. 2010; Sun and Doner 1996). The reaction scheme of a bidentate reaction at low pH and a single monodentate reaction at higher pH (Eqs. 6–7) was also investigated to demonstrate that inclusion of the second monodentate reaction was warranted. For the bidentate binuclear complexes, two approaches are possible based on the exponent for [≡NOH] in the mass action law ($n = 1$ or 2, Eq. 6). A value of $n = 1$ (standard state = 1 mol/L) was used in this study as well as for the previous work for As(V) and PO_4 (Ngantcha-Kwimi and Reed 2016) and implies that the bidentate site is a specific occurrence rather than a random combination of two surface sites (Sigg and Stumm 1991). The coefficient for ≡NOH in the mole balance is 2.

As(III) surface complexation constants determined from a single pH-adsorption edge were used to predict pH-dependent As(III) removal over a range of adsorbate-adsorbent ratios in single, binary, and tertiary adsorbate systems using FITEQ (Herbelin and Westall 1999). For binary and tertiary adsorbate modeling, surface reactions/complexation constants for As(V) and PO_4 from the previous work were used (Ngantcha-Kwimi and Reed 2016). For both As(V) and PO_4, a bidentate surface reaction at low pH with $n = 1$ and a monodentate reaction at higher pH (Waychunas et al. 1993; Fendorf et al. 1997) (Eqs. 9, 10, 11, and 12, Table 2) were used. As(III) oxidation to As(V) in the presence of activated carbon at high pH was observed in our study as well as in others (Ngantcha et al. 2011; Daus et al. 2004; Gu and Deng 2007) and was accounted for by determining As(III) surface complexation constants using data in which the extent of As(III) oxidation was small (< 10% at pH = 8.5).

3 Results and Discussion

3.1 As(III) Oxidation

Ngantcha et al. (2011) observed that As(III) was oxidized to As(V) in the presence of an iron oxide impregnated activated carbon and demonstrated that the carbon surface alone was required for oxidation to occur when the pH was less than 10. This is consistent with the findings of others who reported that As(III) oxidation by iron oxide alone was negligible at pH < 10 (manning et al. 1998; Sun and Doner 1996). To ascertain the oxidation state of adsorbed arsenic, L-Act was contacted with As(III) between pH = 7.4 and 9.6. At about pH = 8.5, about 10% of the total arsenic was present as As(V) with the amount increasing with pH (Fig. 1). Thus, for As(III) adsorption modeling purposes, adsorption data at pH > 8.5 were not included in the determination of As(III) surface complexation constants.

3.2 As(III) Only

In Fig. 2, the fraction of As(III) removed versus pH is presented for L-Act concentrations ranging from 0.05 to 0.225 g/L at an initial As(III) concentration of 0.013 mM. There was minimal As(III) removal by

Table 1 Aqueous, surface acidity, surface contaminant reactions, and mole balances

Equation #	Reactions/mole balance equations	Log K or Ns
Aqueous speciation for As(III)		
(1)	$H^+ + AsO_3^{-3} \leftarrow\rightarrow HAsO_3^{2-}$	13.41a
(2)	$2H^+ + AsO_3^{3-} \leftarrow\rightarrow H_2AsO_{3-}$	25.52 a
(3)	$3H^+ + AsO_3^{3-} \leftarrow\rightarrow H_3AsO_3^{o}o$	34.74 a
Monoprotic surface site—diffuse layer model (MDLM)		
(4)	$\equiv POH + H_s^+ \leftarrow\rightarrow \equiv POH_2^+$	Log Ka $P = 6.54$; Ns $P = 1.84$ mM
(5)	$\equiv NOH \leftarrow\rightarrow \equiv NO^- H_s^+$	Log Ka $N = -7.93$; Ns $N = 3.20$ mM
As(III), As(V), and PO4 surface reactions		
(6)	$\equiv 2NOH + H_3AsO^3 \leftarrow\rightarrow \equiv N_2HAsO_3 + H_2O$	43.30 (this study)
(7)	$\equiv POH + H_3AsO_3 \leftarrow\rightarrow \equiv PH_2AsO_3 + 2H_2O$	39.24 (this study)
(8)	$\equiv POH + H_2AsO_3^- \leftarrow\rightarrow \equiv PHAsO_3^- + 2H_2O$	32.12 (this study)
(9)	$\equiv POH + HAsO_4^{2-} \leftarrow\rightarrow \equiv PAsO_4^{2-} + H_2O$	19.36b
(10)	$\equiv 2NOH + H_2AsO_4^- \leftarrow\rightarrow \equiv N_2AsO_4^- + 2H_2O$	28.96b
(11)	$\equiv POH + HPO_4^{2-} \leftarrow\rightarrow \equiv PPO_4^{2-} + H_2O$	19.91b
(12)	$\equiv 2NOH + H_2PO_4^- \leftarrow\rightarrow \equiv N_2PO_4^- + 2H_2O$	29.54b

*a*Schecher and McAvoy (2007)

bNgantcha-Kwimi and Reed (2016)

≡POH and ≡ NOH are monoprotic surface sites carrying a positive and negative charge, respectively, H+ s is the activity of the proton at the solid surface

Darco 2040 confirming that As(III) removal was due to the impregnated iron oxide. As(III) removal by L-Act increased from pH 4 to a broad maximum between pH 7 and about 8.5 after which removal decreased. This pattern is in agreement with As(III) removal by other iron impregnated carbons (Ngantcha et al. 2011; Gu and Deng 2007). Decreased As(III) removal at pH > 8.5 is due to the following: (1) increased electrostatic repulsion between the negatively charged surface (L-Act $pH_{zpc} = 7.1$) and $H_2AsO_3^-$, (2) increased concentration of OH^- makes As(III)-OH ligand exchange increasingly less favorable, and (3) increasing amount of As(III) oxidation to As(V) with the resulting As(V) not as absorbable at alkaline pHs (Dixit and Hering 2003; Gu and Deng 2007). The adsorption capacity at pH = 8 was 0.057 mol As(III)/mol Fe which, based on our previous L-Act work, was similar to that for As(V) but

Table 2 $F_{predicted}$ values for single, binary, and tertiary adsorbate experiments

Condition	$F_{predicted}$	
	Avg ± Std	(Range)
As(V) alone (17)	0.32 ± 0.33	(0.01–0.92)
As(III) alone	0.56 ± 0.70	(0.01–1.65)
PO4 alone (17)	0.03 ± 0.02	(0.01–0.05)
As(V)–PO4 (17)	0.86 ± 0.71	(0.21–2.39)
As(III)–PO4	1.97 ± 2.13	(0.23–7.17)
As(III)–As(V)	0.47 ± 0.79	(0.01–2.24)
As(III)–As(V)–PO4	1.46 ± 1.52	(0.01–3.63)
Dixit and Hering (2003)	7.7 ± 11	(1.08–24)
Jain and Loeppert (2000)	4.63 ± 5.28	(0.24–12.27)

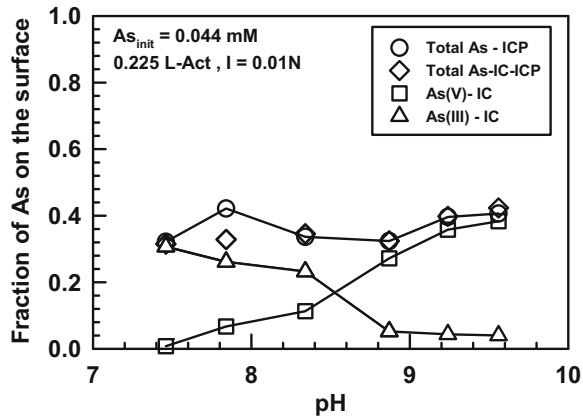

Fig. 1 Speciation of adsorbed As species as a function of pH on L-Act; 0.225 g/L L-Act; 0.044 mM As(III)

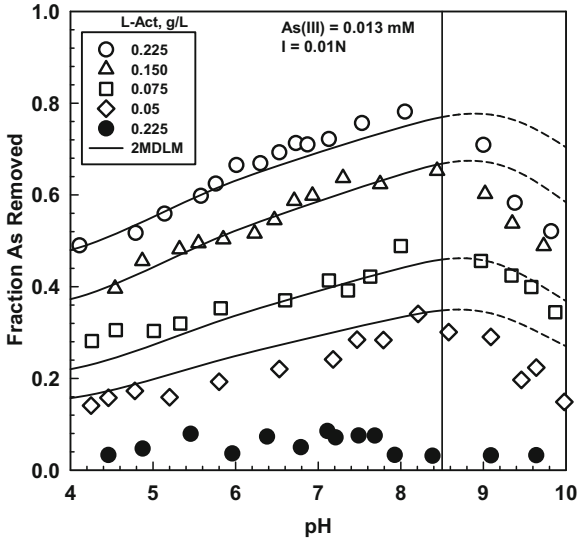

Fig. 2 As(III) sorption as a function of pH and L-Act concentrations; open symbols represent L-Act and closed symbols represent Darco 2040

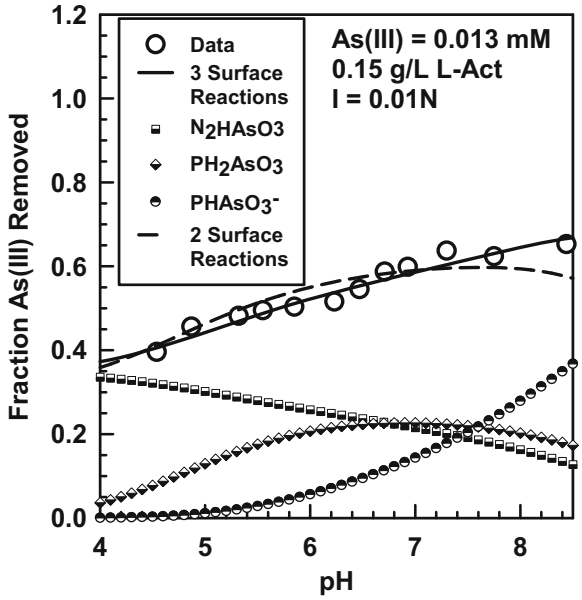

Fig. 3 Speciation of adsorbed As(III) by L-Act as a function of pH; two monodentate and bidentate-monodentate surface species

higher than PO_4 (0.06 mol As(V)/mol Fe; 0.030 mol PO_4/mol Fe) (Ngantcha-Kwimi and Reed 2016). For hydrous ferric oxide (HFO), Pierce and Moore (1982) reported a value of 0.04 mol As(III)/mol Fe, while Dixit and Hering (2003) reported a higher maximum sorption density of 0.31 mol As(III)/mol Fe. Hsu et al. (2008) reported a much lower value of 0.09 mmol As/mol Fe for a reclaimed iron oxide coated sand (9% Fe).

FITEQL fitting results for the pH-adsorption edge at 0.013-mM As(III)-0.15 g/L L-Act are presented in Fig. 3. For the three reaction model, average and maximum differences between model and experimental results were 3% and 5%, respectively with a *FITEQL* F value of 0.1 (F values between 0.1 – 20 indicate a good fit between the data and the model (Herbelin and Westall 1999). Removal by the bidentate site was dominant at low pH (at pH = 4, it was responsible for almost all removal) and was about equal with the monodentate site at pH ≈ 5.2 while at higher pH removal was primarily by the monodentate site. Using two As(III) surface reactions (dotted line) produced a noticeably poorer fit demonstrating that inclusion of the second monodentate surface reaction (Eq. 8; Table 1) was warranted. As(III) surface complexation constants (Log $K^{p}_{H2AsO3-}$ = 32.08; Log K^{p}_{H3AsO3} = 39.26; Log K^{n}_{H3AsO3} = 38.88) determined from the single pH-adsorption edge will be used to predict As(III) removal for the remaining experimental conditions.

For the remaining 0.013 M As(III)-only experiments (Fig. 2) and those at 0.0065 M and 0.026 M As, the 2MDLM accurately predicted the expected decrease in As(III) removal with increasing initial As(III) concentration and decreasing amount of L-Act. In Fig. 2, the 2MDLM predictions were extended beyond pH = 8.5 (dashed line) to demonstrate that the model generally over predicted arsenic removal. This is because of the increasing amount of As(III) oxidation to As(V) with the resulting As(V) not as absorbable.

For L-Act concentrations ranging from 0.05 to 0.225 g/L at 0.013-mM As(III), model predictions were within an average of 4% of experimental data (Fig. 2). For 0.225 g/L and 0.075 g/L L-Act and As(III) concentrations ranging from 0.0065 to 0.026 mM, the predictions were within on average 20% (Fig. 4). In FITEQL (Herbelin and Westall 1999), F values are calculated by

$$F = \frac{\Sigma(Y_i/S_i)^2}{N_p N_c - N_u} \tag{13}$$

where Y_i is the squares of residuals, S_i is the error estimate for each data point, N_p is the number of data points, N_c is the number of components, and N_u is the number of adjustable parameters. For single adsorbate systems, F_{fitted} values were calculated by FITEQL by fitting the complexation constants to individual pH-

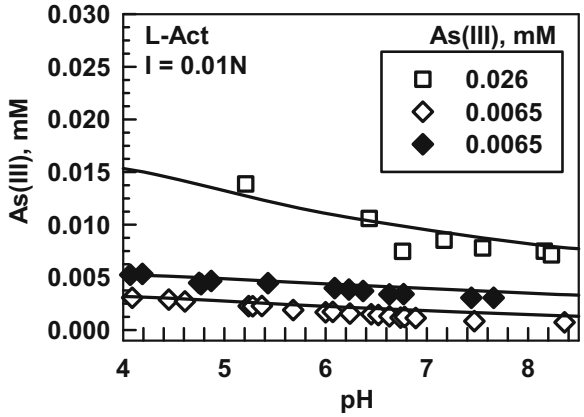

Fig. 4 Equilibrium concentrations of As(III) in single adsorption edges at three initial As(III) concentrations; open symbols represent 0.225 g/L L-Act and closed symbols represent 0.075 g/L L-Act. Lines are 2MDLM predictions

adsorption edge data sets. To assess how close the 2MDLM predictions were relative to the optimized results, $F_{\text{predicted}}$ values were calculated using Eq. 13 with Y_i calculated as

$$Y_i = (\text{2MDLM prediction–experimental data}) \quad (14)$$

The same values of S_i, N_p, N_c, and N_u were used for both F_{fitted} and $F_{\text{predicted}}$, so a comparison can be made. In Table 2, F_{fitted} versus $F_{\text{predicted}}$ are presented for single adsorbate experiments (F values for As(V) and PO_4 were calculated using data from Ngantcha-Kwimi and Reed (2016)). As expected F_{fitted} values were less than $F_{\text{predicted}}$, but the differences between the two values were small demonstrating the 2MDLM's applicability in describing As(III), As(V), and PO_4 removal.

3.3 Binary and Tertiary Adsorbate Systems

The results for the As(III)–As(V) systems are presented in Fig. 5. For the entire As(III)–As(V) data set, $F_{\text{predicted}}$ averaged 0.16 ± 0.23 which indicates the efficacy of the 2MDLM model in predicting competition between As(III) and As(V). At 0.075 g/L L-Act, 2MDLM predictions were within 5% and 13% for As(V) and As(III), respectively, for several As(III)/As(V) molar ratios. At 0.225 g/L L-Act, the total As, As(III), and As(V) are presented. As(V) was better removed than As(III) over the pH range 4 to 8.5; however, the difference in As(V)/As(III) removals decreased with pH (at higher pHs, $[As(V)]_{aq}$ was increasing and $[As(III)]_{aq}$ was decreasing). The vast majority of the total aqueous arsenic was present as the more toxic As(III). The 2MDLM accurately predicted these phenomena (differences were less than 2% for As(V) and within 9% and 8% for As(III) and total As, respectively). It is generally accepted that As(V) is better retained than As(III) by iron oxides at all but high pHs. Ngantcha et al. (2011) reported that As(V) was better removed by FeAC (a different iron-oxide impregnated activated carbon) and Jain and Loeppert (2000) reported similar results for ferrihydrite at similar total arsenic/iron molar ratios between pH 4 and 7.5. At $pH < pH_{zpc}$ it is hypothesized that As(V) is better removed compared with As(III), which exists as a neutral species, because of the electrostatic attraction between the positive surface and the negatively charged As(V).

As(III) results at 1:1 As(III)–PO_4 are presented in Fig. 6 (results for 1:0.5 and 1:2 As/PO_4 molar ratios are presented in SI Fig. S2). There was a good agreement between the 2MDLM predictions and experimental data. At the lowest L-Act concentration (0.075 g/L), the differences between experimental data and model predictions were on average within 15%. At L-Act concentrations of 0.15 g/L and 0.225 g/L, the predictions were within 9% and 15%, respectively. The $F_{\text{predicted}}$ values averaged 1.38 ± 0.75 across the experimental conditions investigated. PO_4 adsorption in the presence of As(III) was also modeled effectively (SI Fig. S3)—model predictions were within 12% of PO_4 experimental data.

As(III) and As(V) results from As(III)–As(V)–PO4 adsorption experiments and 2MDLM predictions are presented in Fig. 7. The 2MDLM successfully predicted the removal of total arsenic, as well as individual arsenic species for 0.075 to 0.225 g/L L-Act. The predictions were within 5% for As(V) and within 14% and 10% for As(III) and total As, respectively, with $F_{\text{predicted}}$ averaging 1.01 ± 1.11. The majority of the aqueous arsenic was present as the more toxic As(III). Additional model validation results are presented in SI Fig. S4 (total As) and Fig. S5 (PO_4). It is important to note that FITEQL did not converge when binary and tertiary data sets were used as inputs to the optimization program reinforcing the necessity of modeling multiple adsorbate systems using the single complexation constant approach.

3.4 Extension of 2MDLM

To demonstrate the robustness of the 2MDLM, adsorption data from Dixit and Hering (2003) (hydrous ferric oxide (HFO)) and Gao and Mucci (2001) (goethite)

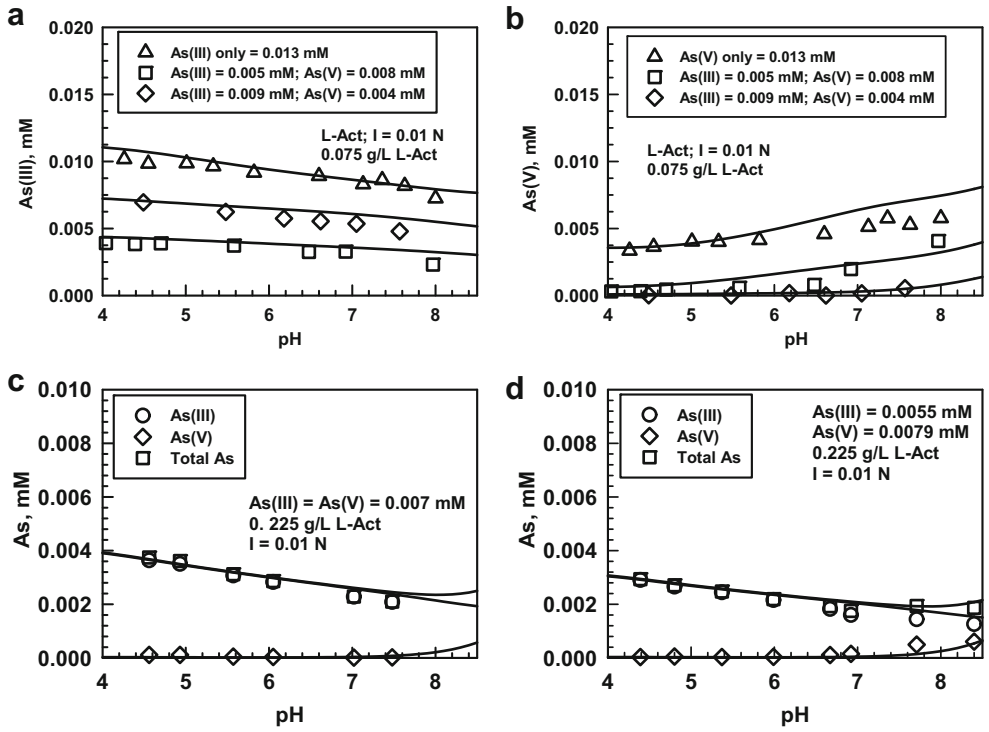

Fig. 5 **a, b** Equilibrium concentrations of As(V)/As(III) in a binary As(III)–As(V)/ adsorbate system on 0.075 g/L L-Act at three different initial As concentrations. **c, d** Equilibrium As(III)/As(V)/total As concentrations as a function of pH in binary As(III)–As(V) adsorbate systems on 0.225 g/L L-Act at two different initial concentrations. Lines are 2MDLM predictions

were modeled. The values of surface area, As(III) and As(V) adsorption densities used in our demonstration were : (1) 600 m^2/g, 0.31 mol As(III)/mol Fe, and 0.24 mol As/mol Fe for Dixit and Hering (2003) and (2) 27 m^2/g, and 0.007 mol sites/mol Fe for Gao and Mucci (2001).

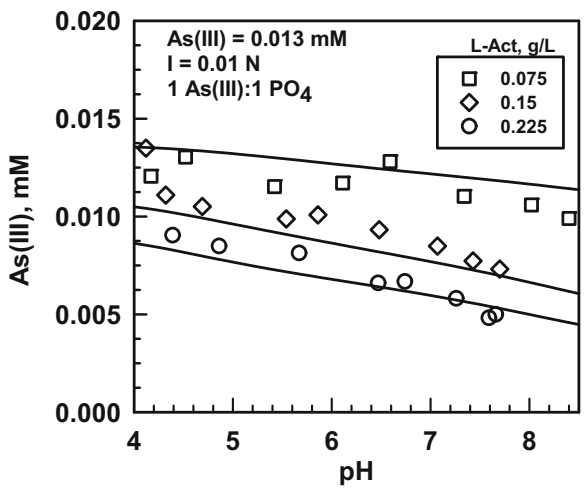

Fig. 6 Equilibrium As(III) concentrations in binary As(III)–PO_4 systems at three different L-Act concentrations. Lines are 2MDLM predictions

In Fig. 8, results from 2MDLM simulations and these authors' experimental data are presented. For Gao and Mucci, the 2MDLM adequately modeled the adsorption of As(V) and the competition between As(V) and PO_4. For Dixit and Hering (2003), single adsorbate behavior and the adverse effect of PO_4 on As(III)/As(V) removal were represented well by the 2MDLM, less so the As(III)-only data (2MDLM predicted essentially no pH effect because of the abundance of surface sites, while experiment data showed that there was a slight dependence on pH). For all conditions studied, the values of $F_{predicted}$ (Table 2) were within the accepted range.

The validity of the 2MDLM in describing adsorption behavior having been demonstrated allows its use in addressing a variety of questions. For illustrative purposes, two examples are given herein. In Fig. S6, competition simulations for differing molar amounts of As(III), As(V), and PO_4 versus an identical increase

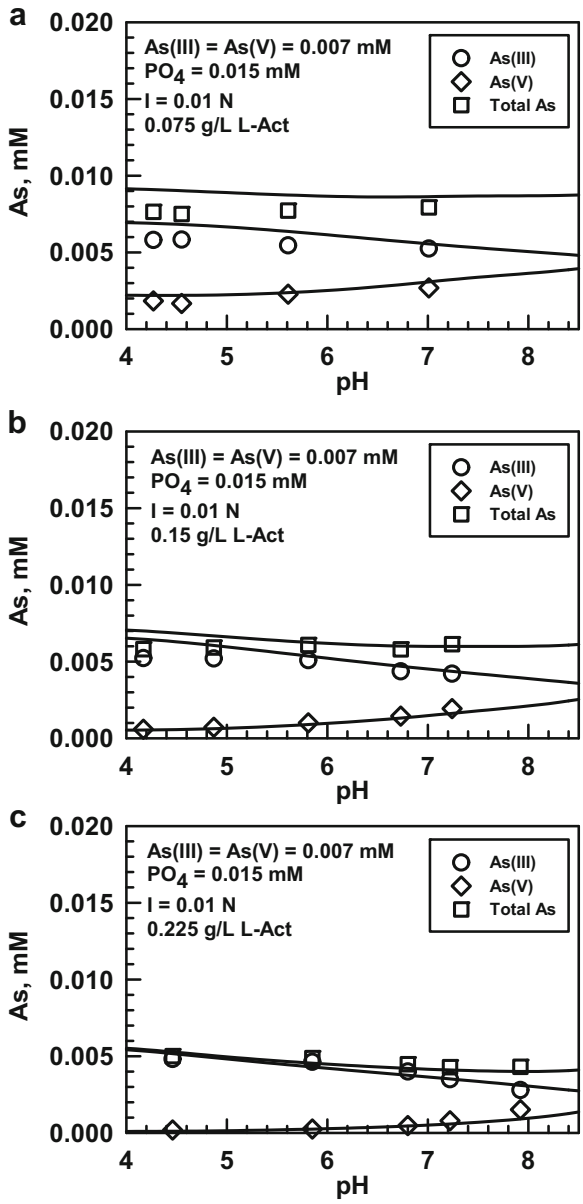

Fig. 7 Equilibrium As(III)/As(V)/total As concentrations as a function of pH in tertiary As(III)–As(V)–PO_4 systems; 1 total As:1 PO_4. **a** 0.075 g/L, **b** 0.15 g/L, and **c** 0.225 g/L L-Act. Lines are 2MDLM predictions

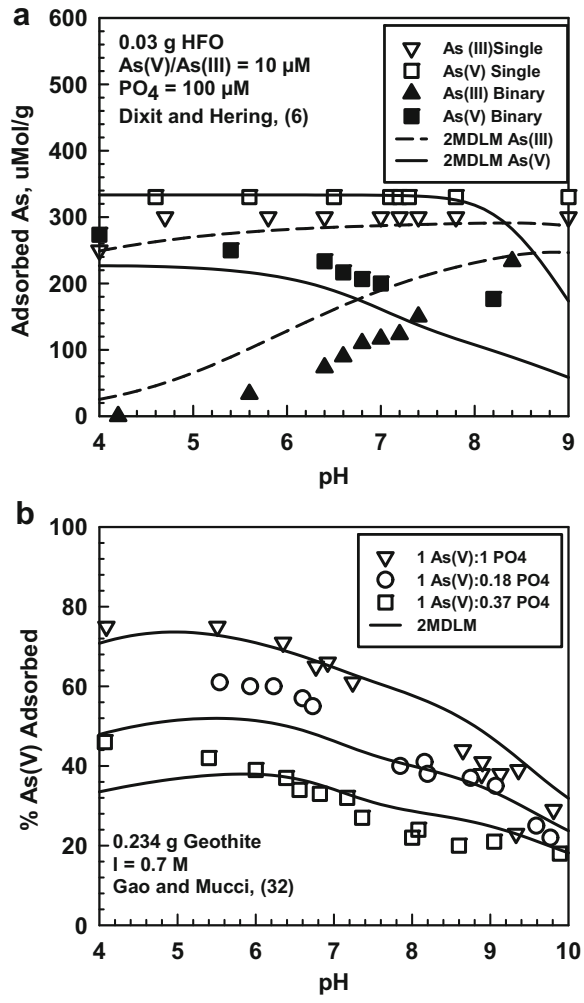

Fig. 8 2MDLM predictions of As(V) and As(III) adsorption edges: **a** 10-μM As(III)/As(V) at 0.03 g/L HFO in single systems and in the presence of 100 μM PO4 and **b** about 9-uM As(V) on 1 g/L goethite in single systems and in the presence PO4. Experimental data from Dixit and Hering[6] and Gao and Mucci[32]

in the adsorbate for a mono-adsorbate system are presented. For As(III), adding an equal molar amount of As(V) decreased As(III) removal significantly more than adding an equivalent amount of As(III). The opposite was observed for As(V)—adding an equal molar amount of As(III) had little effect on As(V) removal relative to adding As(V). Adding an equal molar amount of PO_4 decreased As(III) removal more than an equivalent amount of As(III). For As(V) the opposite was observed—an equal molar amount of As(V) decreased removal more than an equivalent increase of PO_4. The adverse effect of PO_4 was much more pronounced on As(III) than A(V) especially at pH < 8. In Fig. S7, the effects of varying the amount of As(III) and As(V) while keeping the total As constant are presented at pH 6.5 and 8.5. At pH = 6.5, the presence of As(III) significantly decreases total As removal, while at pH = 8.5, the adverse effect is less severe. Simulations of these types can be used to address the merits of As(III) oxidation and pH adjustment as pretreatment steps.

References

Chen, S. L., Dzeng, S. R., & Yang, M. H. (1994). Arsenic species in groundwater's of the blackfoot disease area, Taiwan. *Environmental Science & Technology, 28*(5), 877–881.

Daus, B., Wennrich, R., & Weiss, H. (2004). Sorption materials for arsenic removal from water: a comparative study. *Water Research, 38*, 2948–2954.

Dixit, S., & Hering, J. G. (2003). Comparison of arsenic (V) and arsenic (III) sorption onto iron oxide minerals: implications for arsenic mobility. *Environmental Science & Technology, 37*, 4182–4189.

Dzombak, D. A., & Morel F. M. M. (1987). Adsorption of inorganic pollutants in aquatic systems. *Hydraulic Engineering, ASCE. 113,* 430–475.

Dzombak, D. A., & Morel, F. M. M. (1990). *Surface complexation modeling: hydrous ferric oxide*. New York: Wiley.

Fendorf, S., Eick, M. J., Grossl, P., & Sparks, D. L. (1997). Arsenate and chromate retention mechanisms on goethite surface structure. *Environmental Science & Technology, 31*, 315–320.

Gao, Y., & Mucci, A. (2001). Acid base reactions, phosphate and arsenate complexation, and their competitive adsorption at the surface of goethite in 0.7 M NaCl solution. *Geochimica et Cosmochimica Acta, 64*(14), 2361–2378.

Gu, Z., & Deng, B. (2007). Arsenic sorption and redox transformation on iron-impregnated ordered mesoporous carbon. *Applied Organometallic Chemistry, 21*, 750–757.

Hayes, K. F., Redden, G., Ela, W., & Leckie, J. O. (1991). Surface complexation models: an evaluation of model parameter estimation using FITEQL and oxide mineral titration data. *Journal of Colloid and Interface Science, 142*, 448–469.

Herbelin, A. L., & Westall, J. C. *FITEQL 4.0: a computer program for determination of chemical equilibrium constants from experimental data*, Version 4.0, Report 99–01, Oregon State University, Corvallis, OR 1999.

Hsu, J., Lin, C., Liao, C., & Chen, S. (2008). Removal of As(V) and As(III) by reclaimed iron-oxide coated sands. *Journal of Hazardous Materials, 153*, 817–826.

Jain, C. K., & Ali, I. (2000). Arsenic: occurrence, toxicity and speciation techniques. *Water Research, 34*, 4304–4312.

Jain, A., & Loeppert, R. H. (2000). Effect of competing anions on the adsorption of arsenate and arsenite by ferrihydrite. *Journal of Environmental Quality, 29*, 1422–1143.

Jain, A., Raven, K. P., & Richard, H. (1999). Loeppert. *Environmental Science & Technology, 33*(8), 1179–1184.

James, R. O., & Parks, G. A. (1982). Characterization of aqueous colloids by their electrical double-layer and intrinsic surface chemical properties. *Surface and Colloid Science, 12*, 119–216.

Jang, M., Min, S. H., Kim, T. H., & Park, J. K. (2006). Removal of arsenite and arsenate using hydrous ferric oxide incorporated into naturally occurring porous diatomite. *Environmental Science & Technology, 40*, 1636–1643.

Lumsdon, D. G., Fraser, A. R., Russel, J. D., & Livesey, N. T. J. (1994). *Soil Science, 35*, 381–386.

Manceau, A. (1995). *Geochimica et Cosmochimica Acta, 59*, 3647–3653.

Manning, B. A., Fendorf, S. E., & Goldberg, S. (1998). Surface structures and stability of arsenic (III) on goethite: spectroscopic evidence for inner-sphere complexes. *Environmental Science & Technology, 32*(16), 2383–2388.

Ngantcha, T. A., Vaughan, R., & Reed, B. E. (2011). Modeling As(III) and As(V) removal by an iron oxide impregnated activated carbon in a binary adsorbate system. *Separation Science and Technology, 46*, 1419–1429.

Ngantcha-Kwimi, T. A., & Reed, B. E. (2016). As(V) and PO_4 removal by an iron impregnated activated carbon in a single and binary adsorbate system: experimental and surface complex modeling results. *Journal of Environmental Engineering, 142*(1).

Ona-Guema, G., Morin, G., Wang, Y., Foster, A., Juillot, F., Calsa, G., & Brown Jr., G. (2010). XANES evidence for rapid arsenic(III) oxidation at magnetite and ferrihydrite surfaces by dissolved O2 via Fe2+−mediated reactions. *Environmental Science & Technology, 44*, 5416–5422.

Pierce, M. L., & Moore, C. B. (1982). Adsorption of arsenite and arsenate on amorphous iron hydroxides. *Water Research, 16*, 1247–1253.

Reed, B. E., & Matsumoto, M. R. (1991). Modeling surface acidity of two powdered activated carbons: comparison of diprotic and monoprotic surface representations. *Carbon, 29*(8), 1191–1201.

Reed, B. E., Vaughan, R., & Jiang, L. (2000). Adsorption of heavy metals using iron impregnated activated carbon. *ASCE Journal of Environmental Engineering, 126*(9), 869–874 Research. 34(17), 4304–4312.

Schecher, W. D., & McAvoy, D. C. (2007). *MINEQL+: a chemical equilibrium modeling system, version 4.6*. Hallowell: Environmental Research Software.

Sigg, L., & Stumm, W. (1991). The interactions of anions and weak acids with the hydrous goethite (α - FeOOH) surface. *Colloids and Surfaces, 2*, 101–107.

Smith, E. H. (1998). Surface complexation modeling of metal removal by recycled iron sorbent. *ASCE Journal of Environmental Engineering, 124*, 913–920.

Smith, A. H., Hopenhayn-Rich, C., Bates, M. N., Goeden, H. M., Hertz-Picciotto, I., Duggan, R., Wood, H. M., Kosnett, M. J., & Smith, M. T. (1992). Cancer risks from arsenic in drinking water. *Environmental Health Perspectives, 97*, 259–267.

Stumm, W. (1995). The inner-sphere surface complex. A key to understanding reactivity. In C. P. Huang, C. R. O'Melia, & J. J. Morgan (Eds.), *Advances in chemistry: Vol. 244*, *Aquatic chemistry* (pp. 1–32).

Sun, X., & Doner, H. E. (1996). An investigation of arsenate and arsenite bonding structure on goethite by FTIR. *Soil Science, 161*, 865–872.

US EPA. (2001). National primary drinking water regulations; arsenic and clarifications to compliance and new source contaminants monitoring; final rule. *Federal Register, 66*, 20579–20584.

Vaishya, R. C., & Gupta, S. K. (2003). Arsenic removal from groundwater by iron oxide impregnated sand. *J ASCE Journal of Environmental Engineering, 129*(1), 89–92.

Vaughan, R. L., & Reed, B. E. (2005). Modeling As(V) removal by an iron oxide impregnated activated carbon using the surface complexation approach. *Water Research, 39*(6), 1005–1014.

Vaughan, R. L., Reed, B. E., & Smith, E. H. (2007). Modeling As (V) removal in iron oxide impregnated activated carbon columns. *Journal of Environmental Engineering, 133*(1), 121–124.

Waychunas, G. A., Rea, B. A., Fuller, C. C., & Davis, J. A. (1993). Surface chemistry of ferrihydrite: Part 1. EXAFS studies of the geometry of coprecipitated and adsorbed arsenate. *Geochimica et Cosmochimica Acta, 57*, 2251–2269.

Westall, J., & Hohl, H. (1980). A comparison of electrostatic models for the oxide solution interface. *Advances in Colloid and Interface Science, 12*(4), 265–294.